Manufacturing Rev. **9**, 15 (2022)

https://doi.org/10.1051/mfreview/2022016

Manufacturing Review
Available online at:
https://mfr.edp-open.org

RESEARCH ARTICLE OPEN ACCESS

Optimization of material removal rate and surface characterization of wire electric discharge machined Ti-6Al-4V alloy by response surface method

Deepak Doreswamy[1], D. Sai Shreyas[1], Subraya Krishna Bhat[2,*], and Rajath N. Rao[3]

[1] Department of Mechatronics, Manipal Institute of Technology, Manipal Academy of Higher Education, Manipal, Karnataka 576104, India
[2] Department of Mechanical and Manufacturing Engineering, Manipal Institute of Technology, Manipal Academy of Higher Education, Manipal, Karnataka 576104, India
[3] Department of Mechanical Engineering, NMAM Institute of Technology, Nitte, Karnataka 574110, India

Received: 15 April 2022 / Accepted: 25 May 2022

Abstract. Wire electric discharge machining (WEDM) is one of the foremost methods which has been utilized for machining hard-to-cut materials like Titanium alloys. However, there is a need to optimize their important operating parameters to achieve maximum material removal rate (MRR). The present paper investigates the effect of control factors like current, pulse on time (T_{on}), pulse off time (T_{off}) on MRR of machining of Ti-6Al-4V alloy. The study showed that, increase in current from 2 A to 6 A results in a significant increase in MRR by 93.27% and increase in T_{on} from 20 µs to 35 µs improved the MRR by 7.98%, beyond which there was no improvement of MRR. The increase in T_{off} showed a counterproductive effect. Increase in T_{off} from 10 µs to 30 µs showed an almost linear decrease in MRR by 52.77%. Morphological study of the machined surface showed that cut surface consists of recast layer on which microcracks were present, and revealed the presence of globules, ridge-structured formations of recast layers and voids. In addition, a regression model was developed to predict the MRR with respect to the control factors, which showed a good prediction with an R^2 value of 99.67%.

Keywords: Wire-EDM / material removal rate / ANOVA / peak current / pulse on time / pulse off time

1 Introduction

Titanium and its alloys are extensively used in automobile, petrochemical, aerospace, biomedical, and many other engineering domains due to their attractive mechanical properties such as, superior strength to weight ratio, high corrosion resistance, and their ability to maintain these properties at elevated temperatures [1]. However, their low modulus of elasticity, low thermal conductivity and high chemical reactivity result in large workpiece deflections, drastic cutting temperatures, and significant tool wear rates during machining [2]. Furthermore, their ability to maintain strength at elevated temperatures causes severe work hardening, resulting in extremely high machining forces and vibration related complications such as spring-back and chatter, thus making it difficult to machine using conventional machining techniques [3]. Non-conventional machining techniques provide a better solution while machining such hard materials, but few techniques like Abrasive Water Jet Machining, Electro Chemical Machining, Laser Beam Machining, and Ultrasonic Machining have concerns related to environmental safety during the disposal of chemicals and limitations of affordability to achieve high levels of surface finish [4]. Thus, Wire Electro Discharge Machining (WEDM) is preferred for machining titanium alloys over other machining techniques [5].

In WEDM process, the material is eroded by conversion of electrical energy into thermal energy in the form of spark [6]. The material erosion is made possible by generating recurrent controlled sparks between an electrode (wire) and a work piece to affect only the surface of workpiece. These sparks produce intense heat generating temperature ranging from 8000 °C to 12000 °C. Whenever sparking takes place, a small amount of material is either evaporated or eroded at a minuscule level and flushed away from the work piece by a stream of fluid dielectric medium, which is generally deionized water [6]. While machining using WEDM, a series of input control parameters (process parameters) like pulse on time (T_{on}), pulse off time (T_{off}), wire speed, wire feed rate, wire tension, discharge current, voltage, and dielectric flow rate can be varied to achieve

* e-mail: sk.bhat@manipal.edu

desired output characteristics [7,8]. T_{on} is the discharge time duration, whereas, pulse T_{off} is the time duration of no discharge in between each T_{on} [6]. Wire speed, feed rate, and tension are related to the movement and fixturing of the cutting wire. The current and voltage measure the amount of power spent in discharge machining. The dielectric fluid acts as a coolant preventing excess heat buildup in the work piece, thus reducing one of the difficulties faced during machining hard materials [6].

Optimization of WEDM process parameters is critical to arrive at the required machining performance characteristics. Different optimization techniques such as, Grey Relational Analysis [9], Principle Component Analysis [10], Taguchi method [11,12], Response Surface Methodology (RSM) [13–16], etc., and also combinations of these have been employed to analyze WEDM performance of titanium alloys. The purpose of RSM is to determine the optimum value of the variables at which a particular operation can be performed so as to satisfy certain requirements of output. However, in other optimization methods, many of the times, the optimal values estimated from the mathematical analysis are unrealistic since there is a possibility that the determined combination of process parameters is absent in the machine under consideration [13]. Therefore, RSM has been chosen as the optimization technique in this study.

The influence of wire electrode materials and the dielectric fluid media are important topics of research in the field of WEDM [6]. Materials such as, aluminum, brass, copper, graphite, tungsten carbide, steel, etc., have been employed for the WEDM of titanium alloys [13,17–19]. It has been found that, infusion of copper on graphite [18] and coating zinc on brass [13] results in an improvement in the material removal rate (MRR) of titanium alloys. However, much lesser attention has been paid to the applicability and performance of molybdenum electrode wires on the WEDM of titanium alloys, and their relationship with the operating parameters [20,21]. With regard to the dielectric fluid media, oil and water have been investigated, and water has been found to exhibit higher stability and lower amount of electrode wear rate compared to oil [22]. In the present study, molybdenum was chosen as the electrode material with deionized water being used as the dielectric fluid medium.

Numerous studies have been conducted to study the output performance characteristics such as, slot width (also called kerf width), MRR, and surface roughness (SR), with variations of the major process parameters of WEDM [23,24]. Also, specifically researchers have focused on machining of titanium alloys with WEDM by studying the effect of individual control parameters on the output response characteristics. Among the various parameters that have been investigated, the T_{on}, T_{off} and peak current have received the maximum interest, and their relationships with the material removal rate and surface roughness have been the center of focus [25,26]. With regard to the objective of WEDM performance optimization, investigators have worked on single-response optimization as well as multi-response characteristic optimization techniques using Taguchi's utility and modified utility concepts [27,28]. The findings of these studies have revealed that lower peak currents and higher durations of T_{on} lead to a reduction in the SR, whereas the influence of peak currents on MRR was negligible [29,30]. Other studies have shown that the duration of T_{on} and pulse current are highly influential factors affecting the MRR [31,32].

Fig. 1. Experimental setup.

Machining of titanium alloys is a challenging arena, and WEDM has shown immense potential in this direction. However, the literature shows that there is more scope for understanding the effects of various process parameters of WEDM on the machining performance of titanium alloys. Specifically, the usage of molybdenum wires as the electrode material in combination with deionized water as the fluid medium, and the utilization of RSM in investigating the optimum input process parameters remains to be investigated. Furthermore, very few studies have conducted surface characterization of titanium alloys machined using WEDM and have analyzed the microlevel impact on the machined surface [33], which invariably plays a key part in the structural integrity of the material. Therefore, the core objective of the present study is to investigate the optimum values of the three important WEDM input control factors [34–41], i.e., peak current, durations of T_{on} and T_{off}, for maximizing MRR using molybdenum wire as wire electrode material, while machining Ti-6Al-4V sheet metal through the utilization of optimization techniques like analysis of variance (ANOVA), regression analysis and RSM. Additionally, scanning electron microscopy will be used to perform surface characterization and a morphological analysis of the resulting machined surface of the titanium alloy.

2 Material and methodology

2.1 Experimental setup and workpiece

The machining operation were carried out on Concord CNC Wire-EDM machine (Fig. 1) with table size 320 mm $\times$ 400 mm at Manipal Institute of Technology (MIT) machine tools laboratory, MIT, Manipal Academy of Higher Education, Manipal, India. For the current study, Ti-6Al-4V alloy with dimension 150 mm $\times$ 50 mm $\times$ 2 mm is considered as the work material. Initially, the titanium plate is cut into a slab of the required dimensions (Fig. 2),

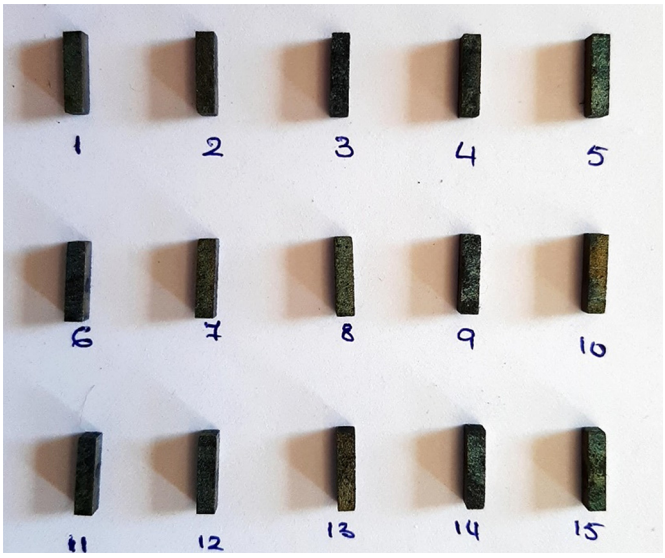

Fig. 2. Wire-EDM machined test samples.

Table 1. Material composition of Ti-6Al-4V.

Chemical composition	Ti	Al	V	Fe	C	Cr	Cu
Percentage	89.54	5.60	4.50	0.23	0.01	0.03	0.09

Table 2. Wire-EDM variable control factors.

Parameters	Unit	Level 1	Level 2	Level 3
T_{off}	µs	10	20	30
T_{on}	µs	20	35	50
Current	A	2	4	6

then machining is carried out by changing some of the process parameters for a length of 10 mm for each trail. Reusable single strand molybdenum metal wire of diameter 0.18 mm is used as wire-electrode and dielectric fluid consisting of cleanser gel, de-ionized water is used for machining of test samples. The material composition of this alloy is presented in Table 1.

2.2 Design of experiments and surface characterization

The wire EDM involves range of control factors such as T_{on}, T_{off}, peak current, wire tension, dielectric fluid composition and its supply pressure, servo voltage, wire speed which influence the machining performance viz., MRR. Based on the results of earlier experiments by the authors [34,35] on different materials using this experimental set up few critical parameters are chosen to determine their influence on the response. It is critical to choose appropriate settings to get the desired or optimum machining performance. In this study, three important control factors T_{on}, T_{off} and peak current are varied in each experiment. The wire speed and tension, dielectric fluid composition and its supply pressure and voltage were set constant throughout the study. For the purpose of optimum utilization of the resources the experiments are designed using central composite design of response surface method. Table 2 shows the variable control factors with values set for the present investigation and Table 3 presents the experimental plan. Material removal rate is basically function of volume removed by machining time. The machining time (T_m) of each slot is taken from the Wire EDM display device. Amount of material removed is determined by weight loss method i.e., difference in weights of test sample before and after machining. Surface morphology of cut surface is studied using scanning electron microscope (Make: Zeiss) and Mitutoyo Inverted metallurgical microscope (Model: IM 7000) is used to study the surface morphology of cut surfaces at different magnification.

3 Results and discussion

3.1 Effect of T_{on}, T_{off} and current on MRR

Experiments are conducted as per the plan shown in Table 4 and the MRR obtained corresponding to each trial is analyzed by computing the average effect of each process

Table 3. Experimental plan.

Std order	Run Order	Blocks	Pt Type	Current (A)	T_{on} (µs)	T_{off} (µs)
1	1	1	1	2	20	20
2	2	1	1	4	35	20
3	3	1	1	2	50	20
4	4	1	1	6	35	10
5	5	1	1	4	20	30
6	6	1	1	6	20	20
7	7	1	1	4	50	30
8	8	1	1	2	35	30
9	9	1	1	4	35	20
10	10	1	1	6	50	20
11	11	1	1	4	35	20
12	12	1	1	2	35	10
13	13	1	1	6	35	30
14	14	1	1	4	50	10
15	15	1	1	4	20	10

Table 4. Computed values of quality characteristics.

S. No.	Current (A)	T_{on} (µs)	T_{off} (µs)	MRR (mm^3/min)
1	2	20	20	0.931
2	4	35	20	1.675
3	2	50	20	1.071
4	6	35	10	3.027
5	4	20	30	1.118
6	6	20	20	2.040
7	4	50	30	1.115
8	2	35	30	0.722
9	4	50	20	1.704
10	6	50	20	1.930
11	4	35	20	1.680
12	2	35	10	1.600
13	6	35	30	1.360
14	4	50	10	2.388
15	4	20	10	2.124

parameters at different levels. Figure 3 shows the main effect plot of different control factors on MRR. From Figure 3a it is observed that with increase of current from 2A to 6 A there is a significant increase in MRR by 93.27%. The increasing trend of MRR is due to increased spark energy at higher current settings [42,43] which led to intensified material vaporization and melting over the larger volume and thus resulted in higher MRR [34,35]. The change in current from 2 A to 4 A, increased the MRR is by 55.96%, but further increase of current from 4 A to 6 A showed that MRR is increased at lower rate (23.96%). This indicated that, increase in current by similar magnitude beyond the peak level reduced the rate of change of MRR.

Further, the effect of T_{on} on MRR is shown in Figure 3b. During T_{on} period, the dielectric fluid gets ionized and spark discharge occurs between wire electrode and the workpiece. This results in the local melting of material from the workpiece and evaporation. It is observed from Figure 3b that with increase in T_{on} from 20 µs to 35 µs the MRR is increased by 7.98% and further increase in T_{on} from 35 µs to 50 µs resulted marginal decrease of MRR by 2.13% compared to its peak MRR which was obtained at $T_{on} - 35$ µs. This is due to the fact that the spark energy is dependent on voltage, current and T_{on}, therefore longer duration of pulse-on time resulting in generating the more intense spark which resulted in melting and vaporization of larger volume of material. But increasing

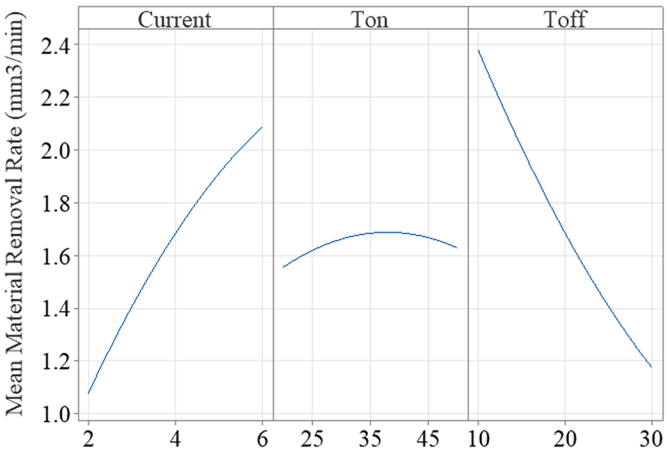

Fig. 3. The effect of current, T_{on} and T_{off} on MRR.

Table 5. ANOVA of MRR.

Source	DF	Adj SS	Adj MS	F-Value
Current	1	2.03434	2.03434	593.74
T_{on}	1	0.01059	0.01059	3.09
T_{off}	1	2.90806	2.90806	848.75
Current × T_{on}	1	0.01553	0.01553	4.53
Current × T_{off}	1	0.15567	0.15567	45.43
T_{on} × T_{off}	1	0.01777	0.01777	5.19
Lack-of-Fit	3	0.01665	0.00555	23.09

DF: degrees of freedom, Adj SS: adjusted sum of squares, Adj MS: adjusted mean squares

the T_{on} duration from 35 µs to 50 µs has resulted in decreasing of MRR by 2.13%. It is well known that there is an increase in spark intensity at T_{on} duration of 50 µs and its corresponding discharge of spark energy led to melting of material with greater volume compared to that of MRR obtained at shorter T_{on}. Since, the T_{off} duration remains same while increasing the T_{on} duration in each spark cycle, there is insufficient time available to evacuate the molten pool from the machining zone during the machining cycle which leave the part of the molten pool as recast layer as seen in Figure 10. Hence longer T_{on} duration beyond the optimum duration shows the decreasing trend of MRR.

The effect of T_{off} on MRR is shown in Figure 3c. Increase in T_{off} from 10 µs to 30 µs has resulted in rapid decrease of MRR by 52.77%. Increasing T_{off} from 10 µs to 20 µs and 20 µs to 30 µs has resulted in decrease of MRR by 31.22% and 31.54% respectively. During T_{off}, the supply of current to electrode is restricted and the dielectric fluid gets deionized, due to which the sparks are not produced. Hence, machining does not take place during T_{off} and MRR decreased almost linearly with increase in T_{off}.

3.2 Analysis of variance of T_{on}, T_{off} and current

ANOVA is used to analyze the significance of the effect of T_{on}, T_{off} and current on MRR at 95% confidence level. F critical values for error degree of freedom − 6 is found to be 2.79 from the standard Fisher's table. Table 5 shows the ANOVA of the control factors on MRR. It is observed for F-value of current and T_{off} is greater than the F critical values and hence its effect is highly significant. It indicates that changes in the settings led to greater variation on MRR. However, the F-value of T_{on} is less than critical F value and hence its effect is not significant. In view of improving the spark frequency and enhancing the MRR, its settings are advised below 35 µs. The interaction effect of these control parameters on MRR is shown in Figure 4. Further, the significance of the interaction effects of these factors are tested by F-test (Tab. 5). The F values of interaction between T_{on} and current, T_{off} and current, T_{on} and T_{off} greater than critical F-values and hence their interaction effects are highly dependent on settings of each other process parameters.

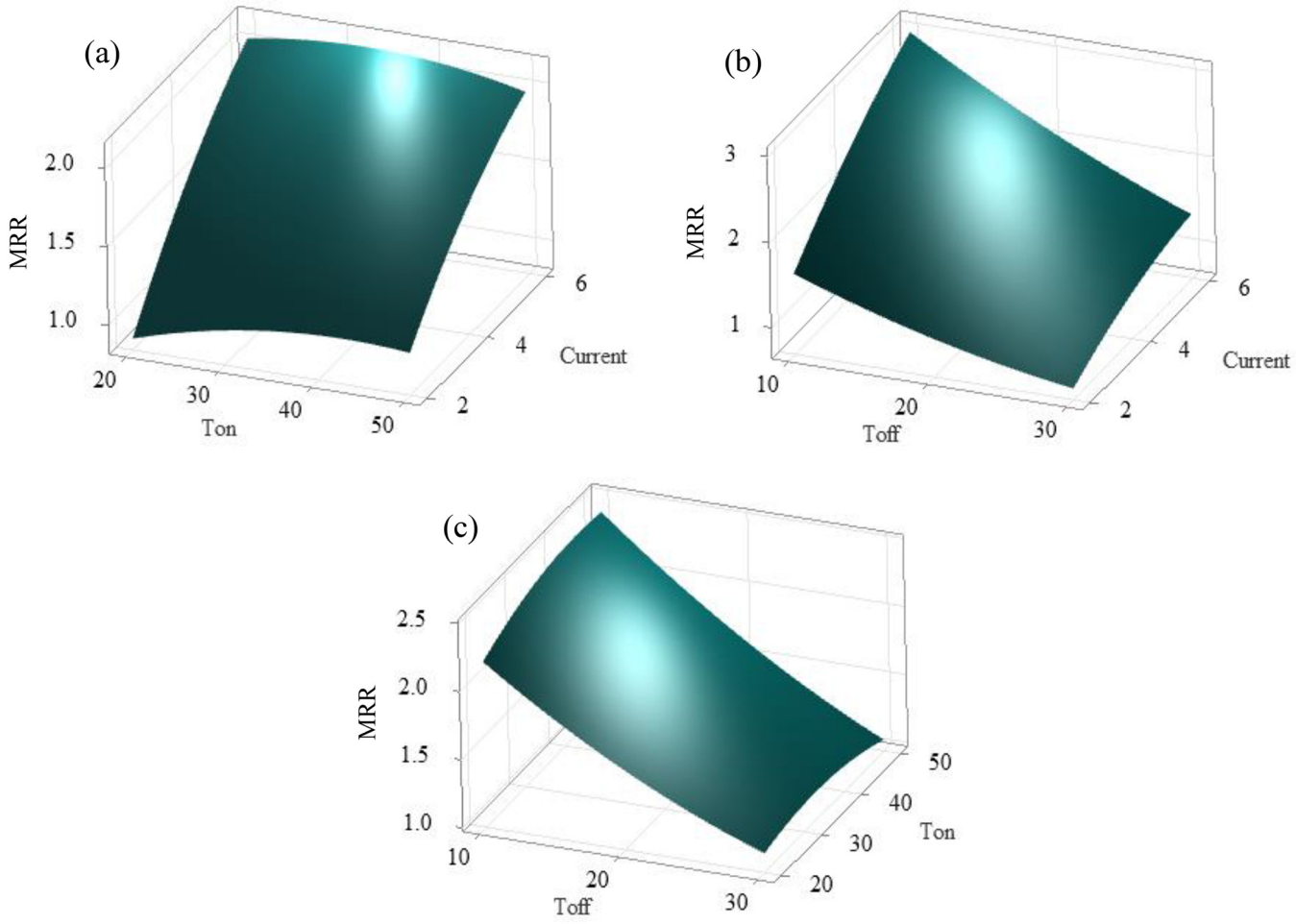

Fig. 4. Interaction effect of (a) $T_{on} \times$ current (b) $T_{off} \times$ current (c) $T_{on} \times T_{off}$.

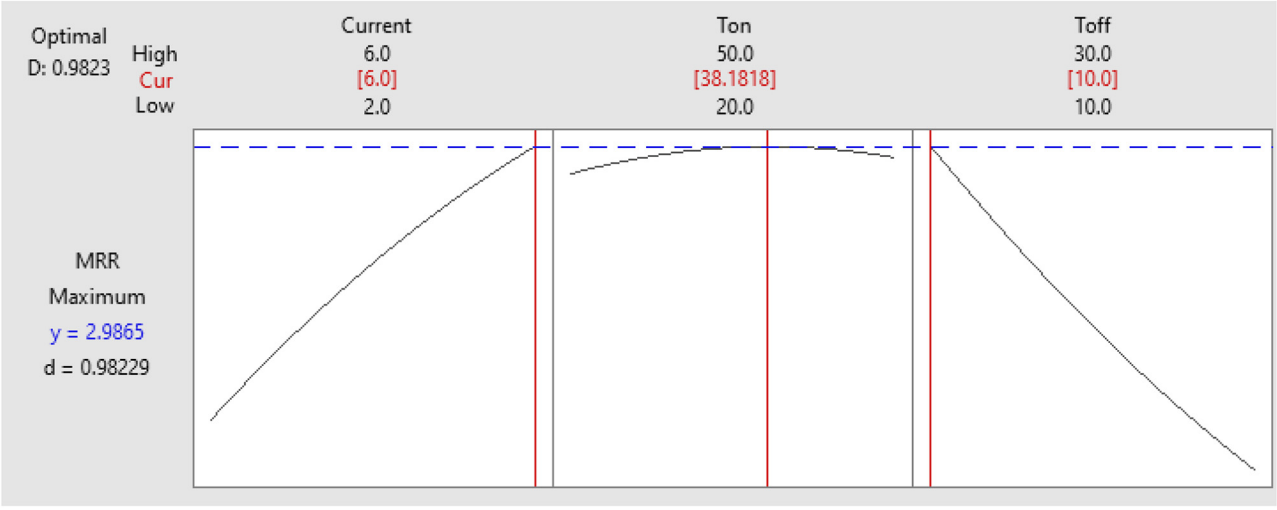

Fig. 5. The optimization plot of MRR.

Table 6. Comparison of predicted and experimental MRR

Trial No.	Current (A)	T_{on} (μs)	T_{off} (μs)	Predicted (mm^3/min)	Experimental (mm^3/min)	Error (%)
1	2	20	10	1.32	1.23	7.42
2	3	25	15	1.58	1.63	3.30
3	4	35	20	1.69	1.53	10.27
4	5	45	25	1.53	1.6	4.57
5	6	50	30	1.20	1.09	9.95
6	6	38.18	10	2.99	2.79	7.04

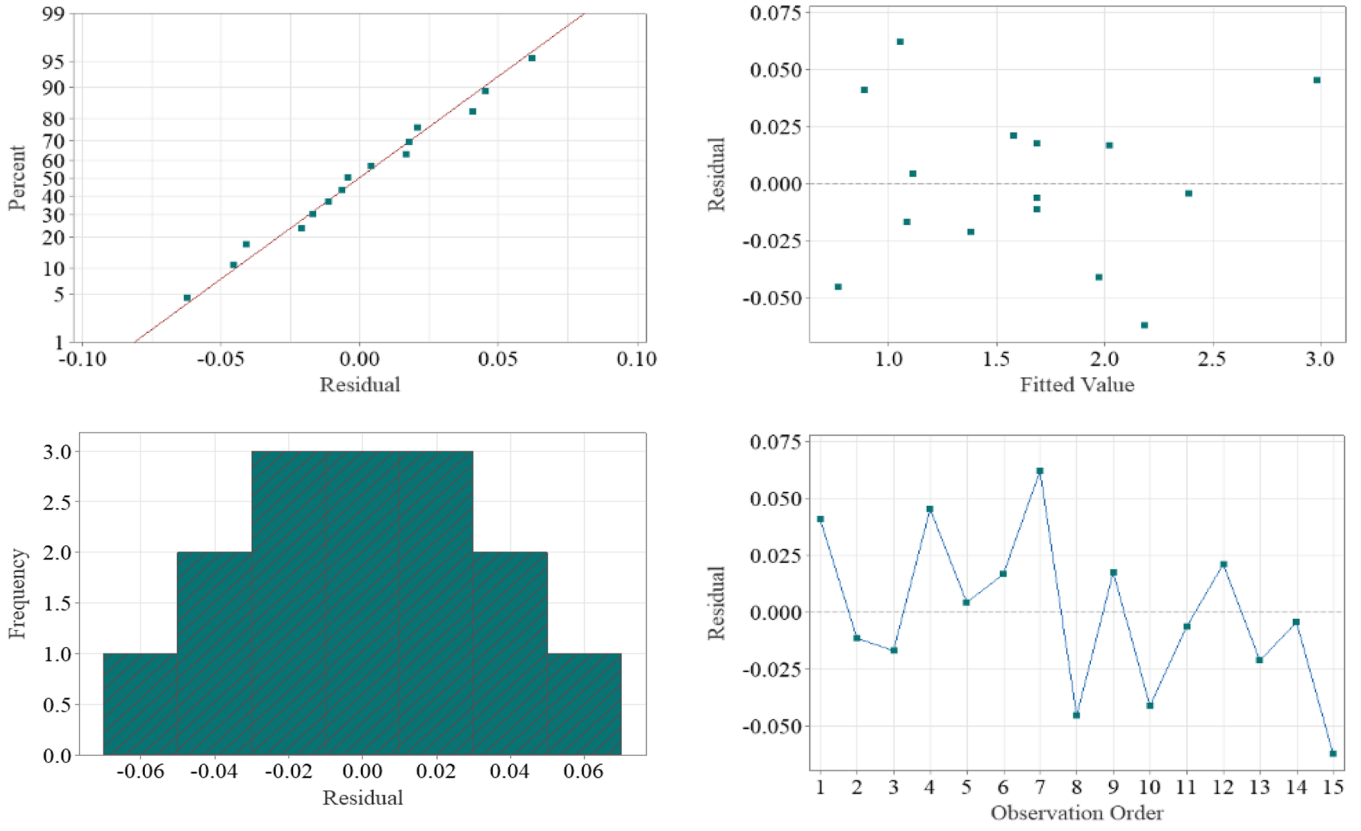

Fig. 6. Distribution of residuals for the developed multivariable nonlinear regression model.

3.3 Analysis of interaction effect by response surfaces

Surface responses are generated for analyzing the effect of variable control factors on MRR. Figure 4a shows the effect of T_{on} and current on MRR. It can be seen that a significant increase on MRR is observed with increasing the T_{on} and current. By keeping T_{on} constant and increasing the current, MRR is significantly increased and the maximum MRR is achieved at $T_{on} - 35$ μs and current $-$ 6 A. Minimum MRR is observed at lowest settings of T_{on} (20 μs) and current (2 A). Figure 4b shows the effect of T_{off} and current on MRR. It is observed that MRR can be increased by increasing the current and decreasing the T_{off}. At any constant settings of current, the MRR can be enhanced by decreasing the T_{off}. From the study it is found that the maximum MRR is achieved at $T_{off} - 10$ μs, current $-$ 6A and also minimum MRR is obtained at current $-$2A and T_{off} $-$30 μs. Figure 4c shows the effect of T_{off} and T_{on} on MRR. It is observed that MRR can be increased by increasing the T_{on} and decreasing T_{off}. By keeping T_{on} constant and decreasing T_{off} MRR is found to be improved. Maximum MRR is achieved at $T_{off} -$ 10 μs and $T_{on} -$ 50 μs and minimum MRR is observed at least value of T_{on} – 20 μs and highest value of $T_{off} -$ 30 μs.

3.4 Optimization of the process parameters

Response surface method is used for optimization of MRR with the objective function of its maximization. Figure 5

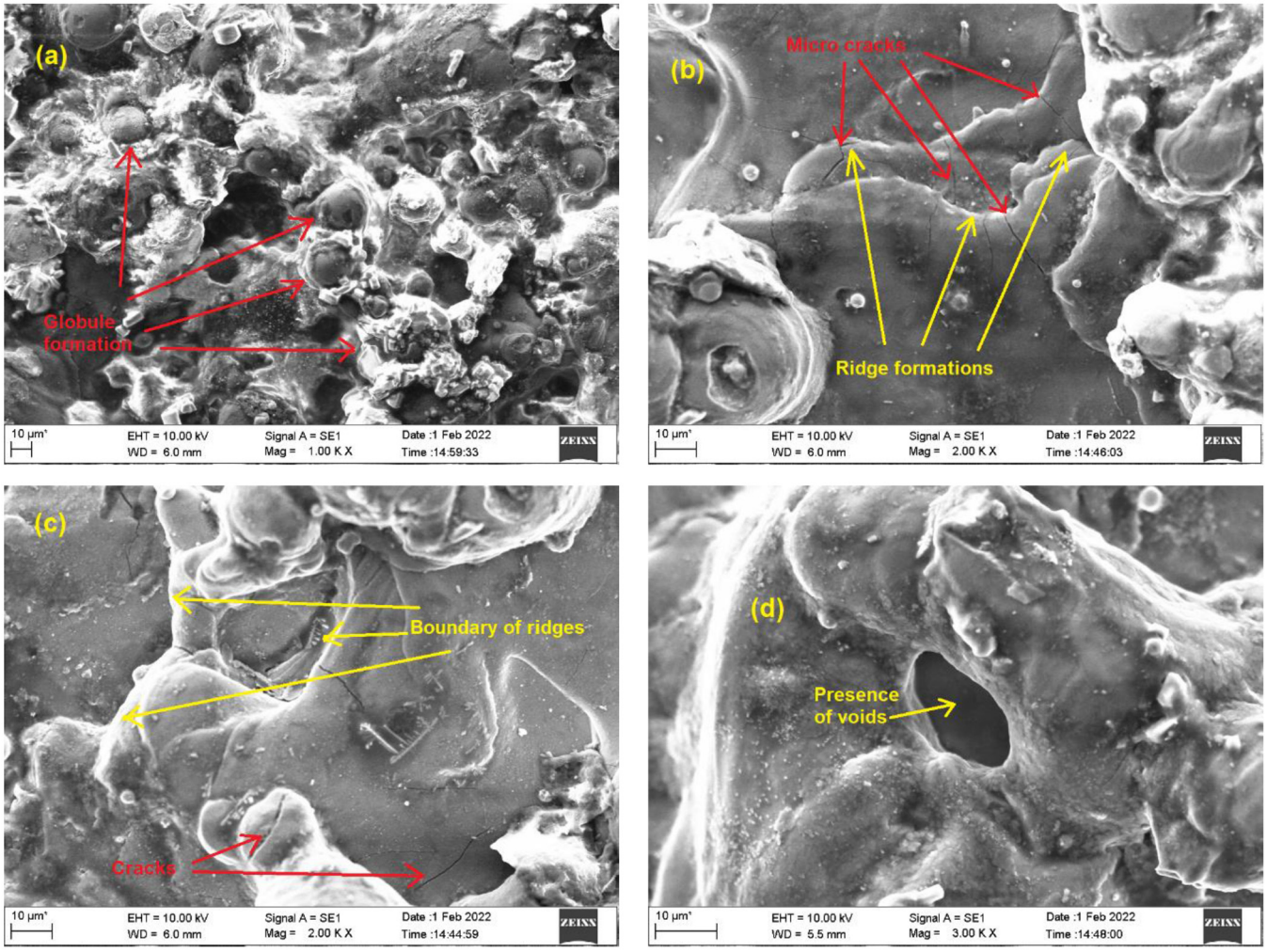

Fig. 7. SEM images of the machined surface showing (a) globule formation at 1000 X, (b), (c) microcracks and ridge formations at 2000 X, and (c) voids at 3000 X magnifications.

shows the optimization plot for MRR. It is observed that, the MRR increases with increase in current. The maximum MRR is seen at settings of 6 A current. Also, the MRR increases with increase in T_{on} up to 38.18 µs, beyond which, it starts decreasing. Further, it is also observed that, highest MRR is achieved at lowest setting of $T_{\text{off}} - 10$ µs. Hence, these settings, i.e., current − 6A, $T_{\text{on}} - 38.18$ µs, $T_{\text{off}} - 10$ µs are the optimized settings to machine the Ti-6Al-4V alloy by Concord CNC Wire-EDM machine using molybdenum electrode. The estimated MRR at these optimized conditions is 2.85 mm^3/min. Considering the limitations of the setting of the experimental machinery, the confirmation experiments were carried out at $T_{\text{on}} - 40$ µs instead of optimized pulse on time of 38.18 µs. This yielded the average MRR of 2.74 mm^3/min.

3.5 Regression modelling of MRR

To establish a relationship between control parameters namely current (I_c), T_{on} and T_{off} with MRR, a regression model is developed using the data shown in Table 4. The model is built based on the experiments conducted for the settings of the control variables in the range: $2\text{ A} \geq I_c \leq 6\text{ A}$, $20\text{ µs} \geq T_{\text{on}} \leq 50\text{ µs}$, $10\text{ µs} \geq T_{\text{off}} \leq 30$. Hence, the developed model is suitable for predicting the MRR within this range. The predictive model of MRR in wire EDM of Ti-6Al-4V is given by equation (1) which is developed in this research. The coefficient of determination (R^2) for the developed model is 99.67%. The predicting accuracy of the regression model is verified with the experimental data. Table 6 shows the confirmation of the prediction capability of the developed model under various operating settings, including the optimum operating condition obtained from the optimization.

$$\begin{aligned} MRR = {} & -0.130 + 0.7241Ic + 0.0483_{Ton} \\ & - 0.0421\text{Toff} - 0.02525I_c^2 - 0.000410T_{on}^2 \\ & + 0.000922T_{\text{off}}^2 - 0.002077Ic \times Ton \\ & - 0.00986Ic \times T_{\text{off}} - 0.000444T_{on} \times T_{\text{off}} \end{aligned} \quad (1)$$

Residual analysis for the MRR is performed and the results are shown in Figures 6a–d. From the probability plot (Fig. 6a), it is observed that the residuals are spread closely across a line of fit. Outlier residual data sets are not found which indicate the good correlation between the predicted and experimental MRR. Figure 6b shows the scatter plot of residuals over the mean value. It is observed that there is no formation of clustered regions of residuals and the residuals are randomly spread across the mean values. This indicates that the robustness of experimental study and the results are not biased. Figure 6c shows the histogram plot of residuals for MRR. It is observed that the frequency distribution of residuals is symmetrical about the mean value and forms the bell-shaped structure indicating the normal distribution of residuals. Figure 6d shows the residual obtained at different experimental trial which show that the residuals are randomly scattered around the mean values. From the residual analysis it is observed that the residuals follow the conditions of linearity, heteroscedasticity and normality. Hence the developed regression model is robust for predicting the MRR within the range of settings: 2 A $\geq I_c \leq$ 6 A, 20 µs $\geq T_{on} \leq$ 50 µs, 10 µs $\geq T_{off} \leq$ 30.

3.6 Analysis of machined surface morphology

Surface characterization of machined Ti-6Al-4V alloy was carried out by scanning electron microscopy (SEM). The machined surfaces at 1000× magnification (Fig. 7a) shows the formation of globules which were intact with the cut surface. The globules were formed during the solidification of molten metal when they are exposed with the dielectric fluid media (deionized water) [44]. Further, the cut surfaces at higher magnification (2000×) exhibited the presence of micro-cracks along the ridge-structured formations [45] as seen from Figures 7b and 7c. The cracks are generated due to rapid cooling of molten metal during the deionization period. Also, it is observed that the solidification of the molten metal resulted in formation of recasts in layered manner, which then adjoin against each other similar to the tectonic plates beneath the earth's crust. Further investigation of microstructure at magnification of 3000× revealed the presence of voids as shown in Figure 7d in between the solidified layer. Similar observations are made by other researchers [46–48]. Such voids are formed due to the inflow of vapors within the microscopic gaps between the molten pool. The average size of such voids was around 22 µm.

4 Conclusions

From the investigation of the effects of peak current, T_{on} and T_{off} on MRR of Ti-6Al-4V using molybdenum electrode, the following conclusions are drawn. Increase in peak current from 2 A to 6 A showed a significant increase in MRR by 93.27%. In case of T_{on}, an increase from 20 µs to 35 µs improved the MRR by 7.98%, whereas its further increase did not show appreciable improvement of MRR. The increase in T_{off} showed a counterproductive effect, i.e., with an increase from 10 µs to 30 µs, there was a linear decrease in MRR by 52.77%. Morphological study of the machined surface showed that cut surface consists of recast layer on which microcracks were present. In addition, SEM images also revealed the presence of globules, ridge-structured formations of recast layer and voids at the microscopic level. At optimum conditions (I_c – 6A, T_{on} – 38.18 µs, T_{off} – 10 µs), the corresponding MRR is 2.74 mm^3/min. Further, the developed regression model can predict the MRR with a good prediction accuracy ($R^2 = 99.67\%$) within the range: 2 A $\geq I_c \leq$ 6 A, 20 µs $\geq T_{on} \leq$ 50 µs, 10 µs $\geq T_{off} \leq$ 30.

Implications and influences

The results derived from the present investigation are useful for predicting the MRR and choosing the optimum process parameter settings for machining of Titanium alloy Ti-6Al-4V in wire-EDM industry. Further, continuing with the present approach, extensive studies can be carried out on other important performance characteristics of WEDM such as surface roughness and kerf width.

Acknowledgments. The authors express their hearty gratitude towards Manipal Institute of Technology, Manipal Academy of Higher Education, for providing the required laboratory facilities to carry out this project.

References

1. S.A. Niknam, R. Khettabi, V. Songmene, Machinability and machining of titanium alloys: a review, in *Machining of Titanium Alloys. Materials Forming, Machining and Tribology*, edited by J. Davim (Springer, Berlin, Heidelberg, 2014), pp. 1–30
2. C. Veiga, J.P. Davim, A.J.R. Loureiro, Review on machinability of titanium alloys: the process perspective, Rev. Adv. Mater. Sci. **34** (2013) 148–164
3. A. Pramanik, Problems and solutions in machining of titanium alloys, Int. J. Adv. Manuf. Technol. **70** (2014) 919–928
4. S.R. Oke et al., An overview of conventional and non-conventional techniques for machining of titanium alloys, Manuf. Rev. **7** (2020) 34
5. B.S. Nishanth, V.N. Kulkarni, V.N. Gaitonde, A review on conventional and nonconventional machining of titanium and nickel-based alloys, AIP Conf. Proc. **2200** (2019) 020091
6. J.A.E. Qudeiri, A.H.I. Mourad, A. Ziout, Electric discharge machining of titanium and its alloys: review, Int. J. Adv. Manuf. Technol. **96** (2018) 1319–1339
7. V.K. Jain, Advanced machining processes (Allied Publishers Pvt. Limited, Edition 6, 2002)
8. S.K. Gauri, S. Chakraborty, A study on the performance of some multi-response optimization methods for WEDM processes, Int. J. Adv. Manuf. Technol. **49** (2010) 155–166
9. J.B. Saedon et al., Multi-objective optimization of titanium alloy through orthogonal array and grey relational analysis in WEDM, Proc. Technol. **15** (2014) 832–840

10. S.O.N. Raj, S. Prabhu, Modeling and analysis of titanium alloy in wire cut EDM using Grey relation coupled with principle component analysis, Aust. J. Mech. Eng. **15** (2017) 198–209
11. M.F. Mohamed, K. Lenin, Optimization of Wire EDM process parameters using Taguchi technique, Mater. Today: Proc. **21** (2020) 527–530
12. F. Nourbakhsh et al., Wire electro-discharge machining of titanium alloy, Proc. CIRP. **5** (2013) 13–18
13. A. Golshan, D. Ghodsiyeh, S. Izman, Multi-objective optimization of wire electrical discharge machining process using evolutionary computation method: effect of cutting variation, Proc. Inst. Mech. Eng. B: J. Eng. Manuf. **229** (2015) 75–85
14. S.P. Arikatla, K.T. Mannan, A. Krishnaiah, Parametric optimization in wire electrical discharge machining of titanium alloy using response surface methodology, Mater. Today: Proc. **4** (2017) 1434–1441
15. R. Chaudhari et al., Multi-response optimization of WEDM parameters using an integrated approach of RSM-GRA analysis for pure titanium. J. Inst. Eng. (India) Ser. D. **101** (2020) 117–126
16. K. Fuse et al., Integration of fuzzy AHP and fuzzy topsis methods for wire electric discharge machining of titanium (Ti6Al4V) alloy using RSM, Materials **14** (2021) 7408
17. A. Hascalik, U. Caydas, Electrical discharge machining of titanium alloy (Ti-6Al-4V), Appl. Surf. Sci. **253** (2007) 9007–9016
18. K. Sivakumar, R. Gandhinathan, Establishing optimum process parameters for machining titanium alloys (Ti6Al4V) in spark electric discharge machining, Int. J. Eng. Adv. Technol. **2** (2013) 201–204
19. A. Uthirapathi, D.L. Singaravelu, Effect of rotating tool electrode on machining of titanium alloy using electric discharge machining, Adv. Mater. Res. **651** (2013) 448–452
20. R. Chaudhari et al., Effect of WEDM process parameters on surface morphology of nitinol shape memory alloy, Materials **13** (2020) 4943
21. K. Fuse et al., Integration of fuzzy AHP and fuzzy TOPSIS methods for wire electric discharge machining of titanium (Ti6Al4V) alloy using RSM, Materials **14** (2021) 7408
22. Obara et al., Study of electrical discharge machining of titanium, J. Jpn. Soc. Electr. Mach. Eng. **39** (2005) 9236–9241
23. M. Manjaiah et al., Influence of process parameters on material removal rate and surface roughness in WED-machining of Ti50Ni40Cu10 shape memory alloy, Int. J. Mach. Machinab. Mater. **18** (2015) 36–53
24. N. Sharma, T. Raj, J.K. Kumar, Parameter optimization and experimental study on wire electrical discharge machining of porous Ni40Ti60 alloy, J. Eng. Manuf. **231** (2015) 1–15
25. V.N. Kulkarni et al., Multi performance characteristics optimization in wire electric discharge machining of Nitinol superelastic alloy, Mater. Today. Proc. **5** (2018) 18857–18866
26. S. Narendranath et al., Experimental investigations on performance characteristics in wire electro discharge machining of Ti50Ni42. 4Cu7. 6 shape memory alloy, Proc. Inst. Mech. Eng. Part B: J. Eng. Manuf. **227** (2013) 1180–1187
27. M. Manjaiah et al., Influence of process parameters on material removal rate and surface roughness in WED-machining of Ti50Ni40Cu10 shape memory alloy, Int. J. Mach. Mach. Mater. **18** (2016) 36–53
28. S. Daneshmand et al., Optimization of electrical discharge machining parameters for Niti shape memory alloy by using the Taguchi method, J. Marine Sci. Technol. **22** (2014) 506–512
29. M. Manjaiah, S. Narendranath, S. Basavarajappa, Wire electro discharge machining performance of TiNiCu shape memory alloy, Silicon **8** (2016) 467–475
30. M.A. Moudood, A. Sabur, M.Y. Ali, I.H. Jaafar, Effect of peak current on material removal rate for electrical discharge machining of non-conductive Al2O3 ceramic, Adv. Mater. Res. **845** (2014) 730–734
31. V. Gaikwad, V.S. Jatti, Optimization of material removal rate during electrical discharge machining of cryo-treated NiTi alloys using Taguchi's method, J. King Saud Univ. Eng. Sci. **30** (2018) 266–272
32. M. Manjaiah et al., Investigation on material removal rate, surface and subsurface characteristics in wire electro discharge machining of Ti50Ni50-xCux shape memory alloy, Proc. Inst. Mech. Eng. Part L: J. Mater. Des. Appl. **232** (2018) 164–177
33. N.K. Gupta et al., Revealing the WEDM process parameters for the machining of pure and heat-treated titanium (Ti-6Al-4V) alloy, Materials **14** (2021) 2292
34. D. Doreswamy, J. Javeri, Effect of process parameters in EDM of D2 steel and estimation of coefficient for predicting surface roughness, Int. J. Mach. Mach. Mater. **20** (2018) 101–117
35. D. Deepak et al., Optimisation of current and pulse duration in electric discharge drilling of D2 steel using graphite electrode, Int. J. Automot. Mech. Eng. **15** (2018) 5914–5926
36. V.K. Meena, M.S. Azad, Grey relational analysis of micro-EDM machining of Ti-6Al-4V alloy, Mater. Manuf. Proc. **27** (2012) 973–977
37. C.H. Huang, A.B. Yang, C.Y. Hsu, The optimization of micro EDM milling of Ti-6Al-4V using a grey Taguchi method and its improvement by electrode coating, Int. J. Adv. Manuf. Technol. **96** (2018) 3851–3859
38. D. Devarajaiah, C. Muthumari, Evaluation of power consumption and MRR in WEDM of Ti-6Al-4V alloy and its simultaneous optimization for sustainable production, J. Braz. Soc. Mech. Sci. Eng. **40** (2018) 400
39. A.V.S. Ram Prasad et al., Multi-response optimization of machining process parameters for wire electrical discharge machining of lead-induced Ti-6Al-4V alloy using AHP-TOPSIS method, J. Adv. Manuf. Syst. **18** (2019) 213–236
40. S.A. Sonawane, B.P. Ronge, P.M. Pawar, Multi-characteristic optimization of WEDM for Ti-6Al-4V by applying grey relational investigation during profile machining, J. Mech. Eng. Sci. **13** (2019) 6059–6087
41. D. Devarasiddappa, M. Chandrasekaran, Experimental investigation and optimization of sustainable performance measures during wire-cut EDM of Ti-6Al-4V alloy employing preference-based TLBO algorithm, Mater. Manuf. Proc. **35** (2020) 1204–1213
42. N. Lenin et al., Optimization of process control parameters for WEDM of Al-LM25/Fly Ash/B4C hybrid composites using evolutionary algorithms: a comparative study, Metals **11** (2021) 1105
43. V. Aggarwal et al., Empirical investigations during WEDM of Ni-27Cu-3.15Al-2Fe-1. 5Mn based superalloy for high temperature corrosion resistance applications, Materials **13** (2020) 3470
44. S. Arooj, M. Shah, S. Sadiq, Effect of current in the EDM machining of aluminum 6061 T6 and its effect on the surface morphology, Arab. J. Sci. Eng. **39** (2014) 4187–4199

45. K.T. Chiang, F.P. Chang, D.C. Tsai, Modeling and analysis of the rapidly resolidified layer of SG cast iron in the EDM process through the response surface methodology, J. Mater. Proc. Technol. **182** (2007) 525–533
46. L. Li et al., Surface integrity characteristics in wire-EDM of Inconel718 at different discharge energy, Proc. CIRP 6 (2013) 220–225
47. B. Xu, M.Q. Lian, S.G. Chen, Combining PMEDM with the tool electrode sloshing to reduce recast layer of titanium alloy generated from EDM, Int. J. Adv. Manuf. Technol **117** (2021) 1535–1545
48. A. Sahu, S.S. Mahapatra, Surface characteristics of EDMed titanium alloy and AISI 1040 steel workpieces using rapid tool electrode, Arab. J. Sci. Eng. **45** (2020) 699–718

Cite this article as: Deepak Doreswamy, D. Sai Shreyas, Subraya Krishna Bhat, Rajath N. Rao, Optimization of material removal rate and surface characterization of wire electric discharge machined Ti-6Al-4V alloy by response surface method, Manufacturing Rev. **9**, 15 (2022)